

# The protective effect of baicalin on duck hepatitis A virus type 1-induced duck hepatic mitochondria dysfunction by activating nuclear erythroid 2-related factor 2/antioxidant responsive element signaling pathway

Linglin Su, Rui Wang, Tianxin Qiu, Jinli Wang, Jinwu Meng, Jinyue Zhu, Deyun Wang, Yi Wu, and Jianguo Liu<sup>1</sup>

*MOE Joint International Research Laboratory of Animal Health and Food Safety and Institute of Traditional Chinese Veterinary Medicine, College of Veterinary Medicine, Nanjing Agricultural University, Nanjing 210095, P R China*

**ABSTRACT** Duck hepatitis A virus type 1 (DHAV-1) is the main pathogen of duck viral hepatitis, but the efficacy of the licensed commercial vaccine needs to be further improved. Therapeutic measures of specific drugs for DHAV-1-infected ducklings need to be urgently developed. Baicalin possesses good antiviral effects. This study aims to investigate the mechanism of baicalin in protecting hepatic mitochondrial function from DHAV-1. The ELISA method was used to detect changes of hepatic and mitochondrial catalase (CAT), superoxide dismutase (SOD), glutathione peroxidase (GPX), inducible nitric oxide synthase (iNOS), adenosine triphosphate (ATP), and malondialdehyde (MDA) levels in vivo and vitro. Hematoxylin and eosin sections and transmission electron microscopy were used to observe liver pathological changes and mitochondrial structural changes. The changes in mitochondrial membrane potential were detected by JC-1 staining method. Western blot and quantitative real-time PCR were employed to analyze the gene and protein expressions in the nuclear erythroid 2-related factor 2 (Nrf2)/antioxidant responsive element (ARE) pathway in duck embryonic hepatocytes infected with DHAV-1. Results showed the administration of baicalin increased the

survival rate of ducklings, and alleviated hepatic damage caused by DHAV-1 by enhancing the antioxidant enzyme activities of the liver and mitochondria, including SOD, GPX, CAT, and reducing lipid peroxidative damage (MDA content) and iNOS activities. The mitochondrial ultrastructure changed and the significant increase of ATP content showed that baicalin maintained the structural integrity and ameliorated mitochondrial dysfunction after DHAV-1 infection. In vitro, DHAV-1 infection led to loss of mitochondrial membrane potential and lipid peroxidation and decreased antioxidative enzyme activities (SOD, GPX) and mitochondrial respiratory chain complex activities (succinate dehydrogenase, cytochrome c oxidase). Baicalin relieved the above changes caused by DHAV-1 and activated the gene and protein expressions of Nrf2, which activated ARE-dependent genes including heme oxygenase-1 (HO-1), nicotinamide adenine dinucleotide phosphate quinone oxidoreductase 1 (NQO1), SOD-1, and GPX-1. In addition, baicalin increased the protein expressions of antioxidative enzymes (SOD, GPX). Hence, baicalin protects the liver against oxidative stress in hepatic mitochondria caused by DHAV-1 via activating the Nrf2/ARE signaling pathway.

**Key words:** DHAV-1, baicalin, Nrf2/ARE, mitochondria, hepatoprotection

2021 Poultry Science 100:101032  
<https://doi.org/10.1016/j.psj.2021.101032>

## INTRODUCTION

Duck hepatitis A virus (DHAV), the major causative agent of duck viral hepatitis (DVH), has been further

divided into 3 serotypes or genotypes, including DHAV-1, DHAV-2, and DHAV-3 (Wang et al., 2008). Of these 3 DHAV types, the most virulent and widespread is DHAV-1, which can cause mortality of up to 95% in young ducklings within 1 wk of age (Kamomae et al., 2017). Beginning in 2013, 2 officially approved live-attenuated vaccines against DHAV-1 strains (CH60 and A66) had been widely used to vaccinate breeder ducks in China (Wen et al., 2018). Due to inadequate protection of the vaccine, DVH still occurred,

© 2021 Published by Elsevier Inc. on behalf of Poultry Science Association Inc. This is an open access article under the CC BY-NC-ND license (<http://creativecommons.org/licenses/by-nc-nd/4.0/>).

Received December 12, 2020.

Accepted January 21, 2021.

<sup>1</sup>Corresponding author: [liujianguo@njau.edu.cn](mailto:liujianguo@njau.edu.cn)

even on farms where vaccination had been implemented (Kang et al., 2018).

There is an urgent need to find specific drugs or active ingredients for DHAV-1 infection.

Recently, upregulation of these antioxidant enzymes by chemical or natural products has become a common strategy to protect cells in the disease. Baicalin exhibits a wide variety of health enhancing biological effects such as anti-inflammatory, antioxidant, antitumor, and antibacterial activities (Oo et al., 2018). As one of the ingredients in traditional Chinese medicine, baicalin has attenuated oxidative stress in vitro and increased the expressions of anti-inflammatory genes (Chen et al., 2017). Additionally, baicalin inhibited DHAV-1 replication by suppressing protein translation (Chen et al., 2018a). Previous reports demonstrated that baicalin treatment conspicuously promoted the expression level of mitochondrial dynamics and prevented mitochondrial dysfunction during *Mycoplasma gallisepticum* infection (Ishfaq et al., 2019).

It has been demonstrated that DHAV-1 could activate the mitochondrial apoptotic pathway through decreasing the mitochondrial membrane potential (MMP) (Lai et al., 2019). Mitochondrial disruption tends to provoke and aggravate liver disorders and it is a common link in most hepatic diseases (Auger et al., 2015). Previous studies had documented that oxidative stress led to the disruption of mitochondrial metabolism (Jin et al., 2017). The nuclear erythroid 2-related factor 2 (Nrf2)/antioxidant responsive element (ARE) pathway involved in oxidative stress and inflammation is a new potential pharmacological target for the treatment of many diseases (de Freitas et al., 2018). Nrf2 highlights the relevance of this transcription factor in pathophenotypes associated with liver damage (Cuadrado et al., 2018). Mitochondria in hepatocytes are particularly prone to the effects of altered substrate influx along with triggering signaling pathways which may lead to cell injury (e.g., cytochrome c release) or cell protection (e.g., increased adenosine triphosphate [ATP] generation) (Grattagliano et al., 2019). Through the induction of heme oxygenase-1 (HO-1) and nicotinamide adenine dinucleotide phosphate quinone oxidoreductase 1 (NQO1) gene expressions, Nrf2 is capable of maintaining mitochondrial function and promoting the removal of damaged mitochondrial units (Strom et al., 2016). This study aims to determine whether baicalin demonstrates an oxidative protective effect to alleviate mitochondrial dysfunction through the Nrf2/ARE pathway.

Although several studies have investigated the anti-inflammatory and antiviral effects of baicalin, investigation of the antioxidative effects of baicalin on duckling liver based on the perspective of mitochondrial dynamics has not been reported. These issues were the focus of this study to determine the potential of baicalin. Thus, we proposed a new mechanism underlying baicalin therapy of DHAV-1. In the present study, we artificially established the duckling model of DHAV-1 infection followed by observation of ultrastructural changes of hepatic

mitochondria and the detection of the activities of enzymes related to liver injury and antioxidative enzymes. Mitochondrial respiratory chain complexes-related indicators and expression levels of mRNA and proteins were also identified. The purpose was to investigate the roles of baicalin in mitochondrial function during DHAV-1-induced peroxidative damage in ducklings' liver.

## MATERIALS AND METHODS

### Reagents and Virus

ATP assay kit, superoxide dismutase (SOD) assay kit, GSH-PX assay kit, catalase (CAT) assay kit, and inducible nitric oxide synthase (iNOS) assay kit were obtained from Nanjing Jiancheng Bioengineering Institute (Nanjing, China). Mitochondrial extraction kit, cytochrome c oxidase (COX) assay kit, malondialdehyde (MDA) assay kit, and succinate dehydrogenase (SDH) assay kit were purchased from Beijing Solarbio Science & Technology Co., Ltd. (Beijing, China). HiScript III RT SuperMix for qPCR (+gDNA wiper) and ChamQ Universal SYBR qPCR Master Mix were purchased from Vazyme (Jiangsu, China). Dulbecco's Modified Eagle's Medium (DMEM, Hyclone, Logan, UT,) supplemented with penicillin 100 IU/mL, streptomycin 100 IU/mL, and 10% fetal bovine serum was used as a nutritive medium. The concentration of fetal bovine serum in DMEM was replaced to 1% as maintenance medium (MM). D-Hank's solution was used for washing the embryo tissue fragments and cells. Baicalin (85%) was purchased from Shanghai Jieli Biotechnology Co., Ltd. (Shanghai, China). The DHAV-1 (strain LQ<sub>2</sub>) used in the challenge experiments was supplied by the Shandong Institute of Poultry (Shandong, China) and was diluted into 50 tissue culture infectious dose 50 with MM.

### Animals and Treatments

A total of 180 one-day-old cherry valley ducklings were purchased from Chaoyang hatchery. After 5 d of adaptive breeding, ducklings were divided into 3 groups randomly and named as blank control (BC) group (separately reared), virus treatment (VC) group, and baicalin treatment (BA) group. The VC and BA groups were intramuscularly injected with 0.2 mL of DHAV-1 ( $10 \times \text{LD}_{50}$ ,  $\text{LD}_{50}$  is  $2.5 \times 10^{-1}$ ) solution per duckling. The BC group was injected with the same volume of normal saline. One hour after being challenged, the BA group was administered with aqueous baicalin in drinking water at a dose of 3 mg/kg·weight per duckling for 3 d, once a day. The BC and VC groups were orally administered with the same volume of solvent-added solution.

### Clinical Curative Effects of Baicalin

The number of dead ducklings were monitored daily until no death was found. The survival rate in each group was calculated according to the formula: survival

rate (%) = number of surviving ducklings/number of total ducklings  $\times$  100%.

### **Histopathological Evaluation**

Liver tissues were obtained from 5 ducklings in each group at the acute phase (4 and 8 h) and stable phase (54 h) after injecting DHAV-1. These ducklings (15 feathers per group) were also anesthetized with CO<sub>2</sub> and were not included in the survival rate. Liver tissue was stored in paraformaldehyde or 2.5% glutaraldehyde, respectively, for histopathological observation. Sections (5- $\mu$ m thickness) were obtained and stained with hematoxylin and eosin, and then examined under a light microscope (Olympus Corporation, Tokyo, Japan).

### **Mitochondrial Ultrastructure Analysis in Liver Tissue**

The isolated liver tissues were fixed with 2.5% glutaraldehyde for 2 h at least and washed twice with buffer. Then the tissues were fixed with 1% osmium tetrachloride for 2 h and dehydrated gradually with ethanol and acetone. Next, the tissues were embedded with the embedding agent and sliced by Leica EM U37 (Leica, Germany). The contrast was enhanced by staining with uranium dioxane acetate and lead citrate. The mitochondrial ultrastructure damage in liver was analyzed by using transmission electron microscopy and observed with Hitachi TEM-1011 (Hitachi, Tokyo, Japan).

### **Indexes of Liver Injury and Mitochondrial Oxidative Stress In Vivo**

Blood samples and liver tissues were obtained from 5 ducklings in each group at 4, 8, and 54 h after injecting DHAV-1. The samples were centrifuged to collect serum after coagulation. Serum alanine aminotransferase (ALT), aspartate aminotransferase (AST), alkaline phosphatase (ALP), lactate dehydrogenase (LDH), and total cholesterol (T-CHO) levels were determined using enzymatic colorimetric assay kits on an automatic biochemistry analyzer (UniCel Dx C 600 Synchron, Beckman Coulter, Brea, CA). The liver tissues were dissected and homogenized in iced saline immediately. Then, the homogenates were centrifuged at 2,500 *g* for 10 min. The supernatants were collected and stored at  $-70^{\circ}\text{C}$  for posterior hepatic SOD, CAT, glutathione peroxidase (GPX), iNOS activities, and MDA content examination. The ATP levels in liver tissues were measured by using the ATP assay kit, according to the instructions. Liver mitochondrion was isolated by using low-temperature differential centrifugation according to the kit instructions and stored at  $-70^{\circ}\text{C}$  for posterior mitochondrial SOD, CAT, GPX, iNOS activities, and MDA content examination.

### **Preparation of Duck Embryonic Hepatocytes (DEHs)**

Liver tissue from a 14-day-old duckling was minced and digested with 0.20% trypsin. After washing thrice with D-Hank's solution, DEHs were cultured in DMEM at  $37^{\circ}\text{C}$  in a humid atmosphere of 5% CO<sub>2</sub>. The cell seeding density was adjusted to about 0.8 to  $1.2 \times 10^6$  cells/mL. DMEM was removed when the DEHs grew into a monolayer.

### **Detection of Mitochondrial Damage Indexes on DEHs**

DEHs preparation and pre-processing were performed as described above. The mitochondrion was isolated by using low-temperature differential centrifugation according to the kit instructions and stored at  $-70^{\circ}\text{C}$  for posterior mitochondrial SOD, COX, GPX, SDH activities, and MDA content examination. All cells were grown on  $\Phi$ 24 mm circular cell slides (WHB, Shanghai, China) and pre-processed as described above. Then, cell samples were stained with JC-1 (Beyotime Institute of Biotechnology, Shanghai, China) for 20 min in a cell culture incubator and examined by standard epifluorescence microscopy (LSM 710, Zeiss, Germany). Either green fluorescence or red fluorescence was detected. Green fluorescence indicated the uptake of JC-1 monomers. Red fluorescence indicated the presence of J-aggregates. Using a long-pass filter system, which allows the visualization of red and green fluorescence simultaneously, orange fluorescence was detected in regions where both green and red fluorescence coexisted.

### **Quantitative Real-Time PCR Detection of Pathway-Relative mRNA Expression**

DEHs preparation and pre-processing were performed as described above. The quantity and integrity of the total extracted RNA from the collected cells were evaluated with a NanoDrop spectrophotometer. Semi-quantitative analysis of the oxidative indexes was conducted using a real-time PCR instrument (QuantStudio 5 Real-Time PCR System, Applied Biosystems, Foster City, CA). The sequences of the primers were *SOD-1* forward, 5'-CCTGTGGTGTTCATCGGAATA-3'; *SOD-1* reverse, 5'-TTGAACGAGGAAGAGCAAGTA-3'; *GPX-1* forward, 5'-CAGTACATCATCTGGTCGCC-3'; *GPX-1* reverse, 5'-CCTGGATCTTGATGGTTTCG-3'; *Nrf2* forward, 5'-AGCCACTTTATTCTTGCCCTCT-3'; *Nrf2* reverse, 5'-AAAATCATCAATCTCCCTGTCCG-3'; *NQO1* forward, 5'-GGTTCATCCCGTGCTCTCA-3'; *NQO1* reverse, 5'-CGTTCATGTCGCCGTTGATG-3'; *HO-1* forward, 5'-GGTCTCCAGATAGCGAGTGT-3'; and *HO-1* reverse, 5'-CCCAGTTTATGCCCTGTTTA-3'. The reaction parameters were as described above. The results were normalized to  $\beta$ -actin expression levels. The

$2^{-\Delta\Delta CT}$  method was used to analyze relative gene expression data.

### Western Blot Analysis of Pathway-Relative Protein Expression

DEHs were harvested and suspended in the lysis buffer (no. 78510, Thermo Pierce, Waltham, MA) containing halt protease and phosphatase inhibitor cocktail (no. 78440, Thermo Pierce). The concentration of the protein extract was determined by a BCA protein assay kit (Beyotime Institute of Biotechnology). Protein (60  $\mu$ g) was diluted in sample loading buffer and boiled for 5 min. Afterward, the samples were separated by 12% SDS-PAGE and transferred to polyvinylidene difluoride membranes. Subsequently, the membrane was blocked

with Tris buffered saline with Tween containing 5% bovine serum albumin at room temperature for 1 h and incubated overnight with specific primary antibodies (anti-Nrf2, anti-GPX, anti-SOD, anti- $\beta$ -actin), respectively, at 4°C. Then the membrane was washed with Tris buffered saline with Tween and incubated in secondary antibodies at room temperature for 1 h. Finally, Western blot images were visualized using a standard enhanced chemiluminescence system (Bio-Rad Laboratories, Hercules, CA).

### Statistical Analysis

All data were analyzed by IBM SPSS statistics 20.0 software (IBM Corporation, Armonk, NY). Comparisons among the experimental groups were carried out using one-way ANOVA and Duncan's multiple range test was used to analyze the differences. Results were

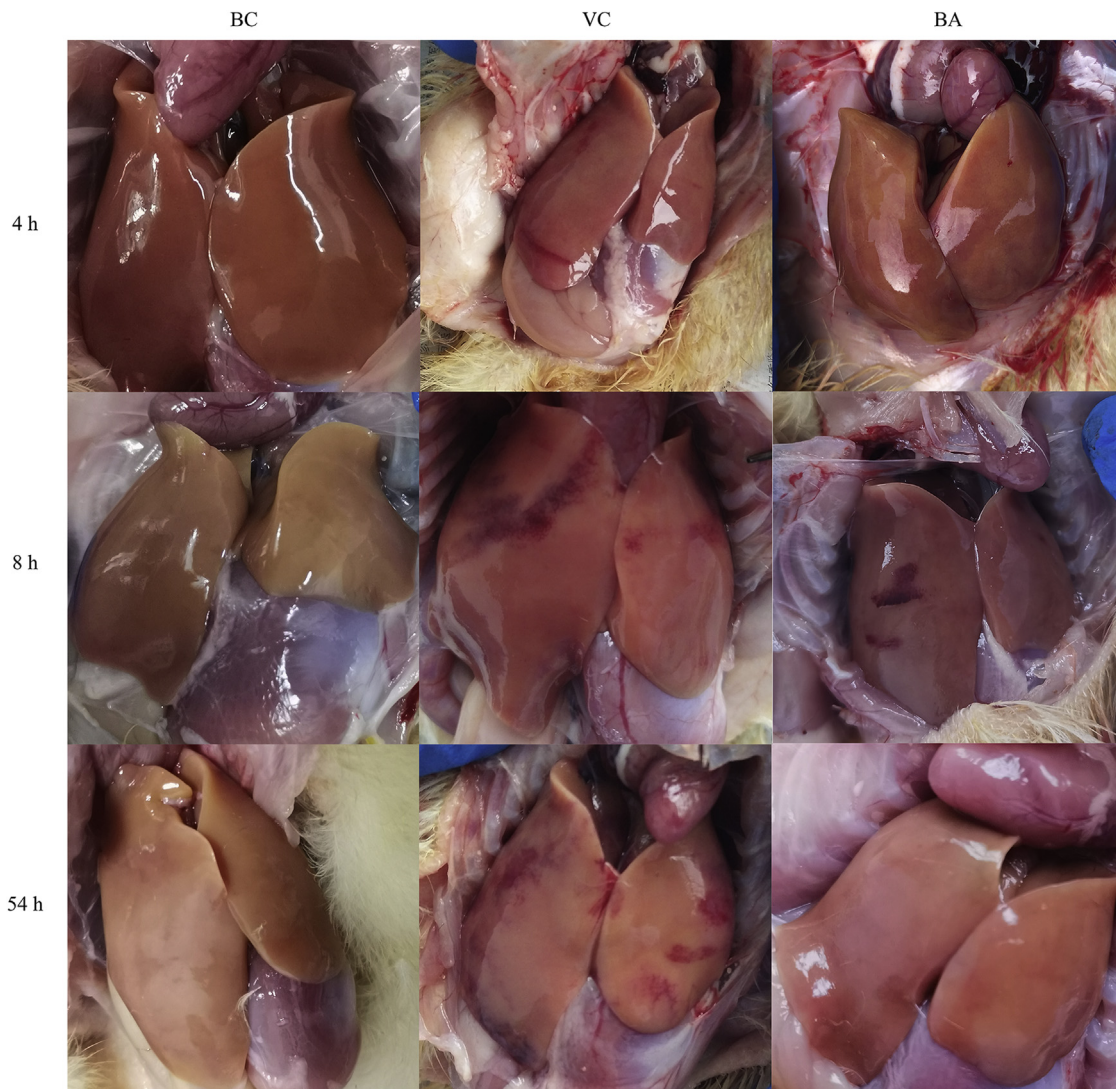


**Figure 1.** Visual assessment of liver pathology. 4, 8, and 54 h mean 4 h, 8 h and 54 h post-injection DHAV-1 solution, respectively. The livers of ducklings in the BC group were normal without pathological changes at the 3 time points. The amount of ecchymosis of the VC group gradually increased from 4 to 54 h. Administration of baicalin in the BA group alleviated the pathological changes induced by DHAV-1. Abbreviations: BA, baicalin treatment after virus incubation; BC, blank control; VC, virus control.

**Table 1.** Changes in liver damage indexes of ducklings.

Index	Time (h)	Group BC	Group VC	Group BA
ALP (U/L)	4	42.65 ± 1.73 <sup>a</sup>	45.74 ± 3.88 <sup>a</sup>	58.57 ± 7.41 <sup>a</sup>
	8	37.38 ± 1.27 <sup>b</sup>	60.34 ± 4.27 <sup>a</sup>	54.55 ± 5.61 <sup>a</sup>
	54	88.88 ± 3.07 <sup>b</sup>	128.14 ± 7.65 <sup>a</sup>	104.07 ± 4.16 <sup>b</sup>
ALT (U/L)	4	16.45 ± 0.84 <sup>a</sup>	28.34 ± 5.37 <sup>a</sup>	25.47 ± 2.56 <sup>a</sup>
	8	15.68 ± 0.69 <sup>b</sup>	26.20 ± 1.64 <sup>a</sup>	23.08 ± 2.10 <sup>a</sup>
	54	16.43 ± 1.68 <sup>b</sup>	61.65 ± 12.85 <sup>a</sup>	28.90 ± 3.10 <sup>b</sup>
AST (U/L)	4	17.73 ± 3.07 <sup>c</sup>	99.97 ± 4.01 <sup>a</sup>	58.87 ± 9.38 <sup>b</sup>
	8	14.21 ± 0.20 <sup>b</sup>	28.44 ± 1.03 <sup>a</sup>	28.96 ± 5.91 <sup>a</sup>
	54	13.70 ± 0.90 <sup>c</sup>	101.48 ± 4.28 <sup>a</sup>	41.87 ± 2.41 <sup>b</sup>
LDH (U/L)	4	97.70 ± 2.02 <sup>b</sup>	281.60 ± 23.59 <sup>a</sup>	122.69 ± 17.92 <sup>b</sup>
	8	106.03 ± 11.84 <sup>b</sup>	235.23 ± 21.58 <sup>a</sup>	65.45 ± 1.46 <sup>b</sup>
	54	133.02 ± 3.32 <sup>b</sup>	862.96 ± 255.17 <sup>a</sup>	176.93 ± 19.70 <sup>b</sup>
T-CHO (mmol/L)	4	4.73 ± 0.59 <sup>a</sup>	4.34 ± 0.19 <sup>a</sup>	4.66 ± 0.10 <sup>a</sup>
	8	5.62 ± 0.35 <sup>a</sup>	6.18 ± 0.17 <sup>a</sup>	6.93 ± 0.80 <sup>a</sup>
	54	6.04 ± 0.42 <sup>a</sup>	3.60 ± 0.28 <sup>b</sup>	5.55 ± 0.39 <sup>a</sup>

<sup>a-c</sup>Data in the same index at the same time point without the same superscripts differ significantly ( $P < 0.05$ ).

Abbreviations: ALP, alkaline phosphatase; ALT, alanine aminotransferase; AST, aspartate aminotransferase; BA, baicalin treatment after virus incubation; BC, blank control; LDH, lactate dehydrogenase; T-CHO, total cholesterol; VC, virus treatment.

expressed as means ± SE.  $P$ -values  $< 0.05$  were considered statistically significant.

## RESULTS

### Clinical Effect and Hepatic Pathologic Changes

The pathological changes in the liver are shown in [Figure 1](#). The livers of ducklings in the BC group were normal without the appearance of pathological changes during the sampling period. In the VC group, ecchymoses could be observed on the surface of the liver 4 h after challenge. From 8 to 54 h, ecchymoses increased and the area expanded gradually. In contrast, results of the BA group were significantly improved, especially at 54 h. The survival rates in BC, VC, and BA groups were 45/45, 7/45, and 14/45, respectively. Administration of baicalin doubled the survival rate compared with the VC group.

### Changes of Liver Injury Indexes In Vivo

[Table 1](#) lists the serum indexes of hepatic injury in each group at different sampling time points after exposure to DHAV-1. At all time points (4, 8, and 54 h), the LDH levels of BC and BA groups tended to be consistent and both were significantly lower than that of the VC group ( $P < 0.05$ ). Difference of the ALP levels among the 3 groups at 4 h was not statistically significant. The ALP levels of VC and BA groups were both conspicuously greater than that of the BC group at 8 h ( $P < 0.05$ ). Until 54 h, baicalin was remarkable for ameliorating the ALP level in the BA group. The trend of the ALT level was similar to that of the ALP level. At 4 h, the AST levels of VC and BA groups were dramatically elevated ( $P < 0.05$ ) and the VC group showed the highest value. At 8 h, the AST levels of the VC and BA groups were remarkably higher than that of the BC group ( $P < 0.05$ ). The trend at 54 h was consistent with that at 4 h. The T-CHO levels were similar among

the 3 groups in the early (4 and 8 h) stages of infection. There was no statistical difference in the T-CHO level between BC and BA groups; both were markedly higher than that of the VC group at 54 h ( $P < 0.05$ ).

### Changes of Hepatic Peroxidative Damage Evaluation Indexes

Results of the hepatic peroxidation indexes are shown in [Figure 2](#). At the early (4 and 8 h) stage, there was an inconspicuous difference in the various indexes among the 3 groups. At 54 h, the CAT, SOD, and GPX levels of the VC group were significantly lower than those of the BC group ( $P < 0.05$ ). However, the iNOS and MDA levels of the VC group were markedly greater than those of the BC group ( $P < 0.05$ ). The SOD and GPX levels of the BA group were remarkably higher than those of the VC group ( $P < 0.05$ ). There was no conspicuous difference in the CAT, iNOS, and MDA levels of the BA group compared with those of the BC or VC group. However, the CAT level of the BA group was higher than that of the VC group and the iNOS and MDA levels of the BA group were lower than those of the VC group.

### Changes of Hepatic Mitochondrial Ultrastructure and ATP Content

Changes in the hepatic mitochondrial structure were observed after 8 h of DHAV-1 exposure ([Figure 3](#)). There was no evidence of mitochondrial damage in the BC group. Compared with the BC group, early swellings could be observed in VC and BA groups; even a vacuolized mitochondrion was visible in the VC group at 8 h. The separation of cristae and clearing of matrix density in the VC and BA groups were also observed. It is worth noting that more marked swelling was accompanied by an architectural disruption in the VC group as the disease progressed. Furthermore, the inner and outer mitochondrial membranes were ruptured and no discernible

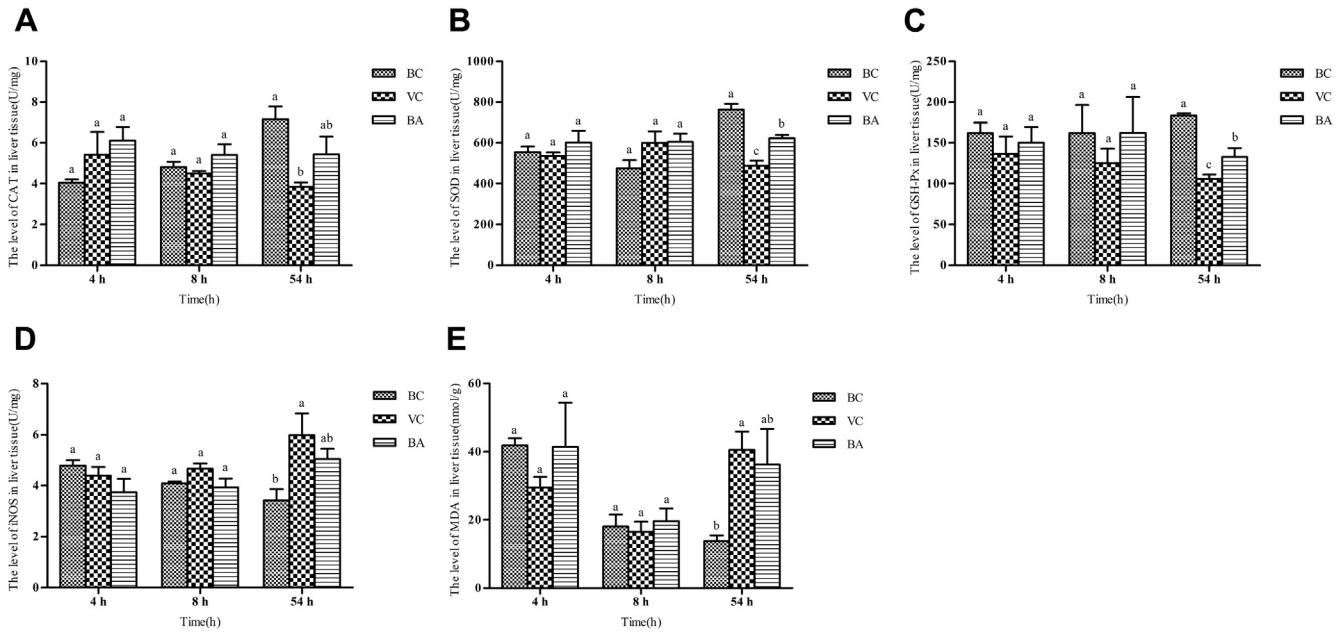


**Figure 2.** Changes of hepatic peroxidation indexes at 4, 8, and 54 h. Liver tissue (A) CAT, (B) SOD, (C) GPX, (D) iNOS activities, and (E) MDA content were detected with the corresponding assay kits. <sup>a</sup>Data without the same superscripts differ significantly ( $P < 0.05$ ). Abbreviations: BA, baicalin treatment after virus incubation; BC, blank control; CAT, catalase; GPX, glutathione peroxidase; iNOS, inducible nitric oxide synthase; MDA, malondialdehyde; SOD, superoxide dismutase; VC, virus control.

regional difference was noted in the degree of severity induced. By contrast, the morphology of mitochondrial was more integrated in the BA group, and manifested by fewer vacuoles and less swelling. As illustrated in Figure 4, the ATP contents of the VC group were significantly lower than those of BC and BA groups at 8 or 54 h ( $P < 0.05$ ).

### Changes of Hepatic Mitochondrial Peroxidation Indexes

To further explore the effects of baicalin on liver function, we tested the indexes related to mitochondrial peroxidative evaluation at 8 and 54 h (Figure 5), including CAT, SOD, GPX, iNOS levels, and MDA content. At 8

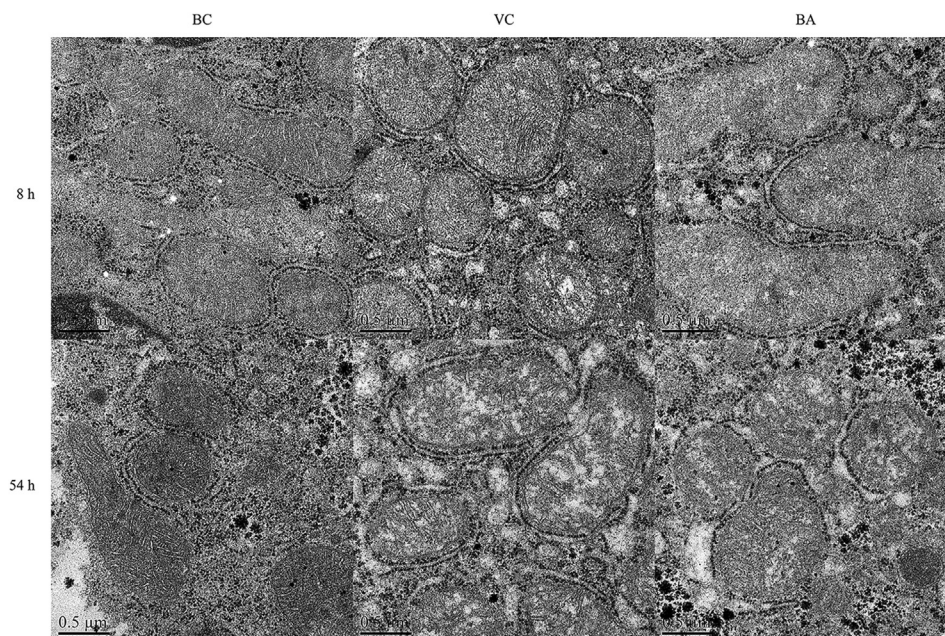


**Figure 3.** Mitochondrial ultrastructure of liver tissue at 8 and 54 h. Liver tissue samples were obtained from individual ducklings of each group at the indicated time points. The changes of mitochondrial ultrastructure were analyzed by using TEM. Scale bar, 0.5  $\mu\text{m}$ . Abbreviations: BA, baicalin treatment after virus incubation; BC, blank control; TEM, transmission electron microscopy; VC, virus control.

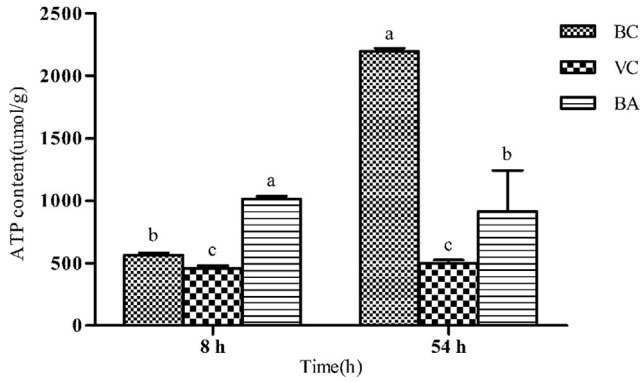


**Figure 4.** ATP content of the 3 groups in liver tissue at 8 and 54 h. The ATP content in liver tissue was detected with an ATP assay kit. <sup>a-c</sup>Bars at the same time points without the same superscripts differ significantly ( $P < 0.05$ ). Abbreviations: ATP, adenosine triphosphate; BA, baicalin treatment after virus incubation; BC, blank control; VC, virus control.

and 54 h, the CAT levels of VC and BA groups were significantly lower than that of the BC group, and the BA group showed significantly higher values than the VC group ( $P < 0.05$ ). The trend of the SOD level was consistent with that of the CAT level. At 8 h, there was an inconspicuous difference in the GPX level of VC and BA groups; both were markedly lower than that of the BC group ( $P < 0.05$ ). Compared with the VC group, the GPX level noticeably increased with the administration of baicalin ( $P < 0.05$ ). At 8 and 54 h, the levels of iNOS and MDA in the VC group were significantly higher than those in the BC group ( $P < 0.05$ ). The iNOS level of the BA group notably increased after the ducklings were exposed to DHAV-1 ( $P < 0.05$ ). Until

54 h, it returned to normal levels due to the effects of baicalin. However, there was no statistical difference in the MDA content of BA and BC groups at 8 h. By 54 h, the MDA content of the BA group was greatly increased but still lower than that of the VC group.

### Changes in MMP of DEHs

To verify the effects of DHAV-1 and baicalin on DEHs mitochondria, we used a fluorescent probe method to detect the MMP. JC-1 has complex spectral properties such that at low concentrations it is monomeric and emits green light, while at high concentrations, there is a spectral shift to red emission due to the so-called “J-aggregate” formation. As **Figure 6** showed, untreated cells (BC group) strongly emitted red fluorescence than green fluorescence, which indicated that the mitochondrial function of the BC group was normal. The cells exposed to DHAV-1 (VC group) had minimal red fluorescence. The administration of baicalin increased the J-aggregate and emitted red fluorescence (BA group). The fluorescence intensity was calculated as the ratio of red fluorescence to green fluorescence by Image J (National Institutes of Health, Stapleton, NY). Results revealed that the BC group was the strongest and VC group was significantly lighter than the other 2 groups ( $P < 0.05$ ).

### Changes of Mitochondrial Peroxidation Indexes In Vitro

Results of the mitochondrial SOD, GPX, and MDA levels in DEHs are presented in **Figure 7**. Mitochondrial SOD activity was significantly reduced when exposed

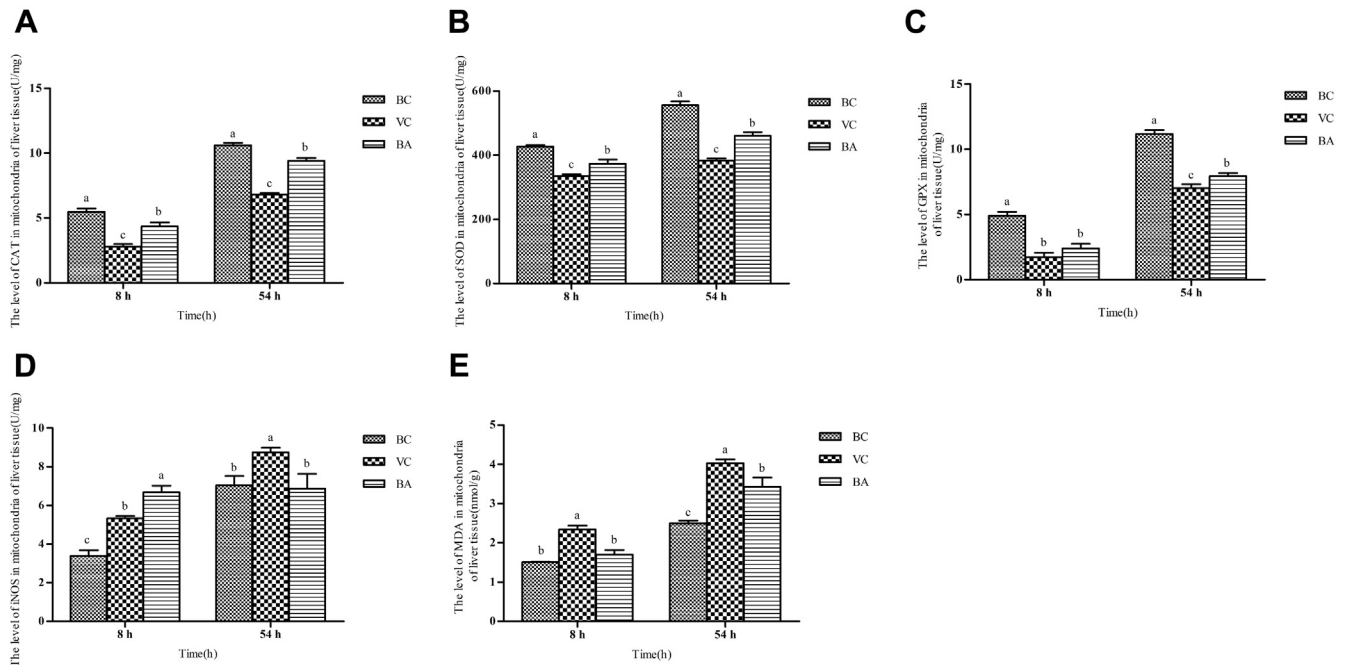


**Figure 5.** Changes of peroxidative evaluation indexes in mitochondria. Liver tissue samples were obtained from individual ducklings of each group at the indicated time points to isolate mitochondria. Then, the mitochondrial (A) CAT, (B) SOD, (C) GPX, (D) iNOS activities, and MDA (E) contents were detected with the corresponding assay kits. <sup>a-c</sup>Bars in the same index at the same time point without the same superscripts differ significantly ( $P < 0.05$ ). Abbreviations: BA, baicalin treatment after virus incubation; BC, blank control; CAT, catalase; GPX, glutathione peroxidase; iNOS, inducible nitric oxide synthase; MDA, malondialdehyde; SOD, superoxide dismutase; VC, virus control.

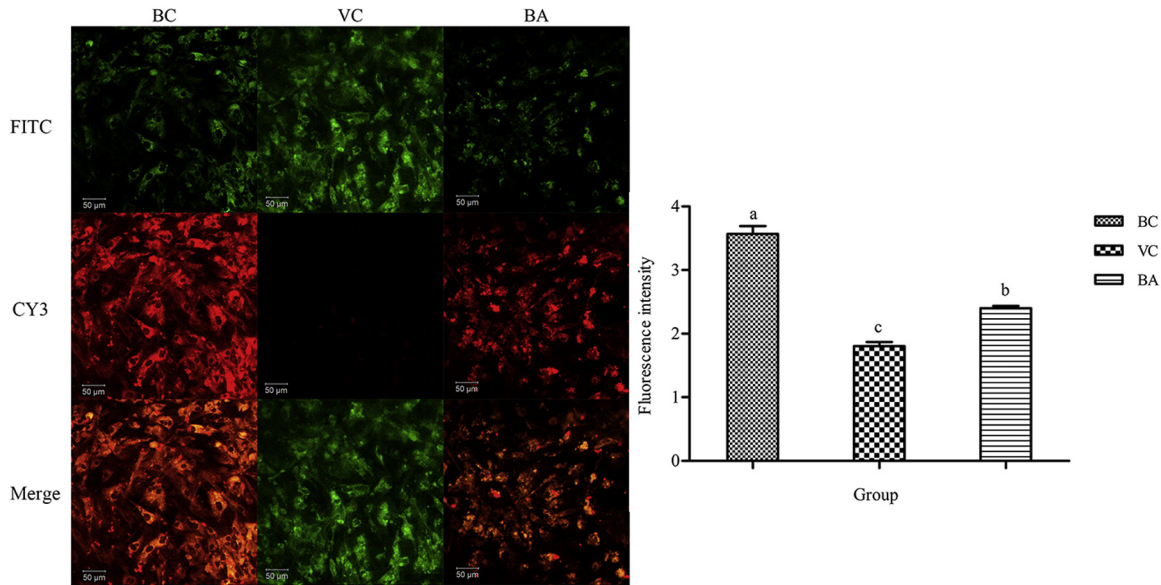


**Figure 6.** Changes of MMP detected by confocal microscopy. Scale bar, 50  $\mu$ m. Double fluorescence staining of mitochondria by JC-1, either as green fluorescent J-monomers (FITC) or as red fluorescent J-aggregates (CY3), was used for monitoring the MMP by standard epifluorescence microscopy. The ratio between the red and green fluorescence of cells loaded with JC-1 was used for the detection of the MMP. There were 3 replicates in each group, and the result was represented by mean  $\pm$  SE. <sup>a-c</sup>Bars without the same superscripts differ significantly ( $P < 0.05$ ). Abbreviations: BA, baicalin treatment after virus incubation; BC, blank control; CY3, cyanine 3; FITC, fluorescein isothiocyanate; MMP, mitochondrial membrane potential; VC, virus control

to DHAV-1 ( $P < 0.05$ ). Under the effect of baicalin, mitochondrial SOD activity noticeably improved as time progressed ( $P < 0.05$ ), which was inconspicuously different from the BC group. At 12 h, the GPX activities among the BC, VC, and BA groups were at the same level and no conspicuous difference was observed. Starting from 24 h, the GPX activities of VC and BA groups reduced significantly, while for the BA group it was evidently higher than the BC group ( $P < 0.05$ ). The GPX activity of the BA group was at the same level as that of the BC group until 36 h. From 12 to 36 h, baicalin downregulated the MDA content compared with the VC group. At 12 and 36 h, the MDA content of the BA group had no statistical differences compared with VC or BC groups.

### Changes on Characteristic Enzymes of Mitochondria In Vitro

As shown in Figure 8, the levels of SDH among BC, VC, and BA groups at 12 h were at the same level and

inconspicuous difference was observed. However, the COX levels of VC and BA groups decreased dramatically compared with the BC group, and the VC group was significantly lower than the BA group ( $P < 0.05$ ). At 24 h, the SDH activities of VC and BA groups were markedly decreased ( $P < 0.05$ ). The COX activities of VC and BA groups were still conspicuously lower than that of the BC group ( $P < 0.05$ ). At 36 h, the SDH and COX levels of the BA group were greatly improved.

### Expression of Nrf2/IARE Signaling Pathway-Related Genes

Table 2 lists the expressions of antioxidant-related genes. The *Nrf2*, *NQO1*, and *HO-1* gene expression levels of VC and BA groups declined sharply, but that of the BA group was significantly greater than the VC group ( $P < 0.05$ ). The *GPX-1* and *SOD-1* gene expressions of the VC group decreased markedly ( $P < 0.05$ ) and baicalin alleviated the downward trend.

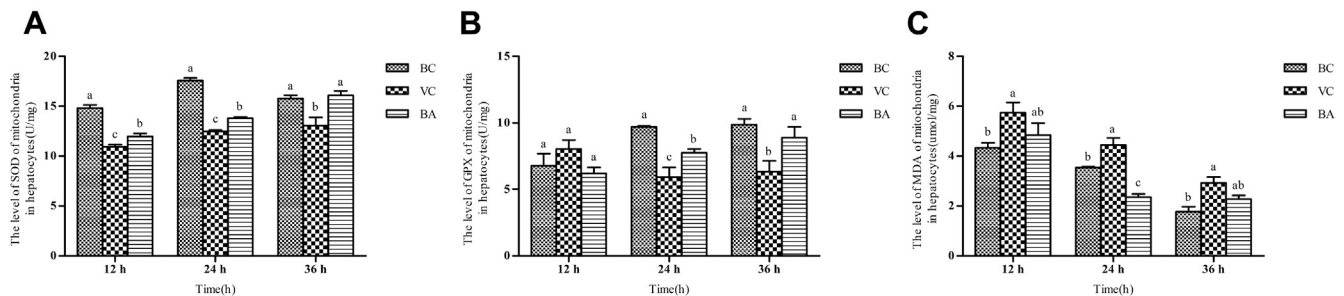


**Figure 7.** Detection of mitochondrial SOD, GPX, and MDA levels at different time points. Mitochondria were isolated from the corresponding cells of different groups. Then the mitochondrial (A) SOD, (B) GPX activities, and (C) MDA content were detected with the corresponding assay kits. <sup>a-c</sup>Bars in the same index at the same time point without the same superscripts differ significantly ( $P < 0.05$ ). Abbreviations: BA, baicalin treatment after virus incubation; BC, blank control; GPX, glutathione peroxidase; MDA, malondialdehyde; SOD, superoxide dismutase; VC, virus control.

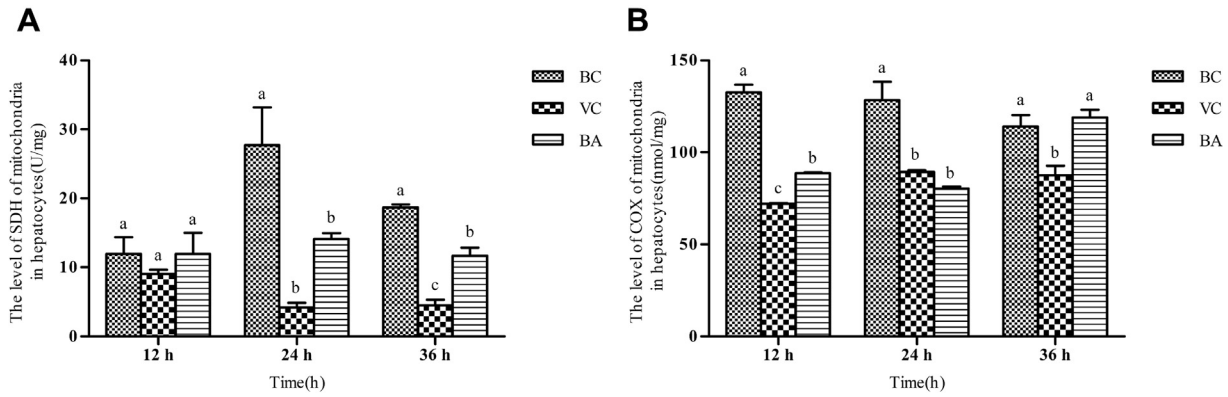


**Figure 8.** Evaluation of the levels of SDH and COX in each group. (A) SDH and (B) COX activities were detected with the corresponding assay kits. <sup>a-c</sup>Bars in the same index at the same time point without the same superscripts differ significantly ( $P < 0.05$ ). Abbreviations: BA, baicalin treatment after virus incubation; BC, blank control; COX, cytochrome c oxidase; SDH, succinate dehydrogenase; VC, virus control.

### Expression of Nrf2/ARE Signaling Pathway-Related Proteins

As shown in Figure 9, the expressions of SOD, GPX, and Nrf2 proteins in VC and BA groups were markedly lower than those in the BC group ( $P < 0.05$ ). However, the detection indexes of the BA group were significantly higher than those of the VC group ( $P < 0.05$ ).

## DISCUSSION

Liver damage is the most typical pathological symptom of DHAV-1 infection. It has been reported that the liver is typically enlarged with petechial and ecchymotic hemorrhages throughout at autopsy which ducklings infected DHAV-1 (Yugo et al., 2016). Baicalin has been proven to reduce hepatic liver oxidative damage in ducklings caused by DHAV-1 infection (Chen et al., 2018b). Based on the experiment in vitro, we designed an animal regression experiment to confirm that baicalin did increase the survival rate of ducklings infected with DHAV-1. More specifically, the survival rate dropped from 15.2 to 30.4%, with a reduced level of liver ecchymosis from visual pathological pictures (Figure 1). Meanwhile, administration of baicalin stabilized the serum hepatic indexes after the acute phase of infection, including ALP, ALT, AST, LDH, and T-

CHO (El-Nekeety et al., 2014; Baradaran et al., 2019), which are widely used indicators to evaluate liver damage caused by hepatitis (Table 1).

Oxidative stress is associated with cell injury by DHAV-1 (Du et al., 2016). In the late stage of DVH infection, it seems that oxidative stress caused severe damage to hepatocytes and aggravated the severity of DVH in the DHAV-1-infected group (Xiong et al., 2014). In our research, the CAT, SOD, and GPX activities in liver tissues at 54 h after injection of DHAV-1 solution were significantly reduced; besides, the iNOS activity and MDA content were significantly increased. Changes of the above-mentioned indexes can be explained by the oxidative stress to the liver caused by DHAV-1, which is consistent with the results of Xiong et al. (2014). MDA is a recognized marker of lipid oxidative decay (Pisoschi and Pop, 2015), which reflects the degree of cell damage. SOD is responsible for the detoxification of superoxide radicals. The product of this reaction called hydroperoxide is toxic, which must be removed from the cell. GPX and CAT are responsible for the detoxification of hydroperoxide by converting it to water (Surai and Kochish, 2019). Meanwhile, iNOS often participates in diverse biological mechanisms, such as regulating mitochondrial functions, apoptosis, and inflammation (Cheng et al., 2017). In our study, SOD, CAT, and GPX activities in liver tissues of ducklings administered baicalin gradually increased; besides iNOS activity and MDA content decreased. These indicators reflect that baicalin can reverse oxidative damage to the liver caused by DHAV-1.

The function of the liver depends on mitochondria producing ATP for biosynthesis and detoxification (Zhang et al., 2019). As a major source of reactive oxygen species (ROS) production, mitochondria also could be the major target of ROS attack (Petrosillo et al., 2007). Here, we proposed a hypothesis that mitochondria were also damaged by oxidative stress caused by DHAV-1. Thus, by comparing the hepatic mitochondrial ultrastructure of the VC group with that of the BA group, we proved that the structural integrity of mitochondria was destroyed in ducklings infected with

**Table 2.** Influence of antioxidant-related gene expression on DEHs.

Index	Group BC	Group VC	Group BA
Nrf2	1.01 ± 0.09 <sup>a</sup>	0.20 ± 0.02 <sup>c</sup>	0.62 ± 0.03 <sup>b</sup>
GPX-1	1.07 ± 0.06 <sup>a</sup>	0.81 ± 0.02 <sup>b</sup>	1.01 ± 0.09 <sup>a,b</sup>
SOD-1	1.01 ± 0.10 <sup>a</sup>	0.58 ± 0.01 <sup>b</sup>	1.07 ± 0.06 <sup>a</sup>
NQO1	1.00 ± 0.02 <sup>a</sup>	0.28 ± 0.01 <sup>c</sup>	0.49 ± 0.09 <sup>b</sup>
HO-1	1.01 ± 0.10 <sup>a</sup>	0.37 ± 0.03 <sup>c</sup>	0.64 ± 0.00 <sup>b</sup>

<sup>a-c</sup>Data in the same index without the same superscripts differ significantly ( $P < 0.05$ ).

Abbreviations: BA, baicalin treatment after virus incubation; BC, blank control; DEHs, duck embryonic hepatocytes; GPX-1, glutathione peroxidase 1; HO-1, heme oxygenase; NQO1, nicotinamide adenine dinucleotide phosphate quinone oxidoreductase 1; Nrf2, nuclear erythroid 2-related factor 2; SOD-1, superoxide dismutase 1; VC, virus treatment.

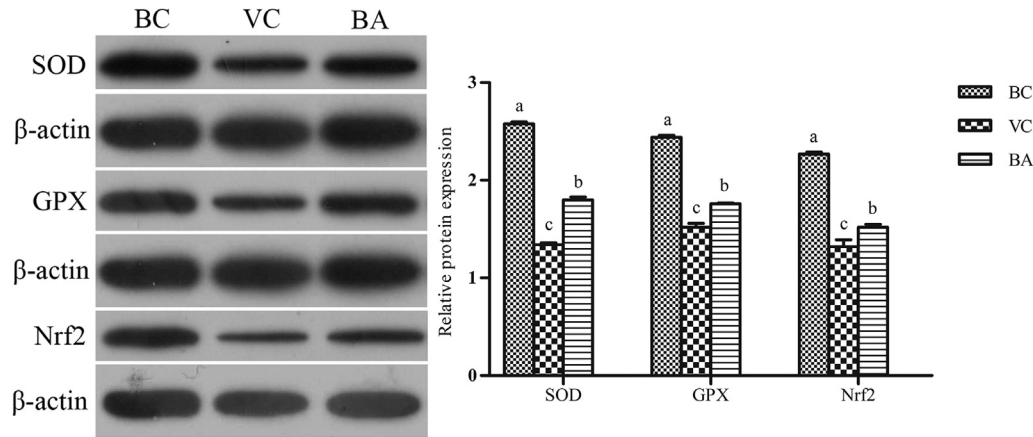


**Figure 9.** Influence of baicalin treatment on cellular SOD, GPX, and Nrf2 expressions. The relative expressions of SOD, GPX and Nrf2 proteins were detected by Western blot. <sup>a-c</sup>Bars in the same index without the same superscripts differ significantly ( $P < 0.05$ ). Abbreviations: BA, baicalin treatment after virus incubation; BC, blank control; GPX, glutathione peroxidase; Nrf2, nuclear erythroid 2-related factor 2; SOD, superoxide dismutase; VC, virus control.

DHAV-1 at 8 and 54 h (Figure 3). As illustrated in Figure 4, we found that the level of ATP production of liver tissue in the VC group was significantly reduced, but administration of baicalin could significantly elevate the level of ATP production over the period from 8 to 54 h. In addition, we found that the changing trend among these groups was consistent with that of liver tissue via evaluating the peroxidative indexes in mitochondria. The results indicated that mitochondria was responsible for damage caused by DHAV-1 and that the damage occurred before hepatocyte and baicalin could improve it.

The above results showed that baicalin had a curative effect on the mitochondrial damage of duckling liver tissue infected by DHAV-1. Does it have a similar effect on the mitochondria of hepatocytes cultured in vitro? What is the pathway of action? The effect of baicalin on mitochondria undergoing DHAV-induced oxidative stress, in vitro, further confirmed our hypothesis. MMP is an indicator of mitochondrial activity and it plays a major role in ATP production, redox balance, signaling, and metabolism (Al-Zubaidi et al., 2019). As shown in Figure 6, the uninfected cells in the BC group had good cell activities and normal MMP with weak green fluorescence and strong red fluorescence. Sporadic distribution of red fluorescence could be observed in the VC group. Noteworthy, MMP gradually recovered in cells incubated with the virus and baicalin of the BA group. It implied that the MMP was attenuated and mitochondrial membrane permeability changed in cells infected by DHAV-1, and baicalin could protect mitochondria from the virus. Our study demonstrated that baicalin gradually increased the mitochondrial SOD and GPX activities in DEHs, which was decreased by DHAV-1 solution (Figure 7). The MDA content of the VC group was always significantly higher than that of the BC group. The effects of baicalin on DEHs revealed a trend of fluctuations in MDA content for 24 h after incubation, but it also stabilized the MDA level. Both the mitochondrial respiratory chain and the electron transport chain

are closely related to enzymes. Larger quantities of NO were released from iNOS during inflammatory or immunological defense reactions and were involved in host tissue damage. NO binds to COX, and thus activates cellular signaling cascades. This action can also lead to the release of superoxide anion from the mitochondrial respiratory chain (Moncada and Bolanos, 2006). SDH is the main source of ROS generation in the mitochondria (Bezawork-Geleta et al., 2017). By detecting the characteristic enzymes on the mitochondrial membrane, SDH and COX, we found that DHAV-1 reduced the SDH and COX activities in DEHs and strongly affected the physiological functions of mitochondria, leading to the accumulation of superoxide. After treatment with baicalin, the SDH activity resumed 24 h post-infection and the COX activity resumed earlier than the SDH activity (Figure 8). Therefore, we established that the antioxidative effect of baicalin not only worked on liver tissue and mitochondria in vivo, but also affected the mitochondria in vitro.

The mechanism of baicalin-mediated protection against oxidative stress remains to be fully elucidated. The Nrf2/ARE signaling pathway is an important mediator of cellular response during an oxidative stress condition (Shaw and Chattopadhyay, 2020). Nrf2 is the key regulator of expression levels for more than 100 genes coding for antioxidants via the ARE located in their upstream promoter region (Deramaut et al., 2013), including *NQO1*, *HO-1*, *SOD-1*, and *GPX*. It was reported that the activity of Nrf2 may profoundly influence health and disease by altering mitochondrial metabolism (Ludtmann et al., 2014). Overexpression of Nrf2 prevented  $H_2O_2$  from inducing changes in the mitochondria of isolated cardiomyocytes, such as disruption of mitochondrial networks, loss of MMP, and decreased expression of cytochrome c (Strom et al., 2016). Genetic activation of Nrf2 increases the mitochondrial membrane potential and ATP levels, the rate of respiration, and the efficiency of oxidative phosphorylation (Holmstrom et al., 2013). To identify the molecular

mechanism related to the attenuation of the DHAV-induced oxidative stress and mitochondrial damage by baicalin treatment, we identified the relative gene and protein expressions of Nrf2/ARE pathway components. Both the gene expression of *Nrf2* and the downstream antioxidant enzymes (GPX-1, SOD-1, NQO1, HO-1) on DEHs were caused by DHAV-1. There was a gradual upward trend of gene expression after treatment by baicalin, especially the increase in *SOD-1* consistent with uninfected cells (Table 2). What's more, the protein expression trends of SOD, GPX, and Nrf2 were consistent with gene expression trends by Western blot (Figure 9). Thus, we conclude that baicalin activated the Nrf2/ARE pathway in DEHs

It is noteworthy that baicalin is still challenging to promote clinical applications due to its low bioavailability (Huang et al., 2019). Since 1984, the outbreak of the DHAV-1 infection in China (Guo Yupu, 1984), pathological symptoms have gradually changed. It has been reported that the liver and pancreas are important target organs for DHAV (Liu et al., 2019). Our research only focused on the liver tissue of DHAV-1-affected ducklings, which exhibited limitations. Furthermore, the current treatment of ducklings suffering from DVH is still unsatisfactory, and the development of vaccines is challenging. Even worse, the emergence of a new viral subtype (Liu et al., 2019) poses a greater threat to breeding farmers.

## ACKNOWLEDGMENTS

This work was supported by the National Natural Science Foundation of China (grant nos. 31772784 and 31572557), and the Project Funded by the Priority Academic Program Development of Jiangsu Higher Education Institutions (PAPD). We thank all other staff at the Institute of Traditional Chinese Veterinary Medicine of Nanjing Agricultural University for their assistance with the experiments.

## DISCLOSURES

The authors declare that there is no conflict of interest.

## REFERENCES

- Al-Zubaidi, U., J. Liu, O. Cinar, R. L. Robker, D. Adhikari, and J. Carroll. 2019. The spatio-temporal dynamics of mitochondrial membrane potential during oocyte maturation. *Mol. Hum. Reprod.* 25:695–705.
- Auger, C., A. Alhasawi, M. Contavadoo, and V. D. Appanna. 2015. Dysfunctional mitochondrial bioenergetics and the pathogenesis of hepatic disorders. *Front. Cell Dev. Biol.* 3:40.
- Baradaran, A., F. Samadi, S. S. Ramezanzpour, and S. Yousefdoost. 2019. Hepatoprotective effects of silymarin on CCl<sub>4</sub>-induced hepatic damage in broiler chickens model. *Toxicol. Rep.* 6:788–794.
- Bezawork-Geleta, A., J. Rohlena, L. Dong, K. Pacak, and J. Neuzil. 2017. Mitochondrial complex II: at the Crossroads. *Trends Biochem. Sci.* 42:312–325.
- Chen, Y., L. Zeng, J. Yang, Y. Wang, F. Yao, Y. Wu, D. Wang, Y. Hu, and J. Liu. 2017. Anti-DHAV-1 reproduction and immuno-regulatory effects of a flavonoid prescription on duck virus hepatitis. *Pharm. Biol.* 55:1545–1552.
- Chen, Y., W. Yuan, Y. Yang, F. Yao, K. Ming, and J. Liu. 2018a. Inhibition mechanisms of baicalin and its phospholipid complex against DHAV-1 replication. *Poult. Sci.* 97:3816–3825.
- Chen, Y., Y. Yang, F. Wang, X. Yang, F. Yao, K. Ming, W. Yuan, L. Zeng, and J. Liu. 2018b. Antiviral effect of baicalin phospholipid complex against duck hepatitis A virus type 1. *Poult. Sci.* 97:2722–2732.
- Cheng, P., T. Wang, W. Li, I. Muhammad, H. Wang, X. Sun, Y. Yang, J. Li, T. Xiao, and X. Zhang. 2017. Baicalin alleviates Lipopolysaccharide-induced liver inflammation in chicken by suppressing TLR4-mediated NF-kappaB pathway. *Front Pharmacol.* 8:547.
- Cuadrado, A., G. Manda, A. Hassan, M. J. Alcaraz, C. Barbas, A. Daiber, P. Ghezzi, R. Leon, M. G. Lopez, B. Oliva, M. Pajares, A. I. Rojo, N. Robledinos-Anton, A. M. Valverde, E. Guney, and H. Schmidt. 2018. Transcription factor NRF2 as a therapeutic target for Chronic diseases: a systems medicine Approach. *Pharmacol. Rev.* 70:348–383.
- de Freitas, S. M., L. Pruccoli, F. Morroni, G. Sita, F. Seghetti, C. Viegas, and A. Tarozzi. 2018. The Keap1/Nrf2-ARE pathway as a pharmacological target for Chalcones. *Molecules* 23:1803.
- Deramandt, T. B., C. Dill, and M. Bonay. 2013. Regulation of oxidative stress by Nrf2 in the pathophysiology of infectious diseases. *Med. Mal. Infect.* 43:100–107.
- Du, H., S. Zhang, M. Song, Y. Wang, L. Zeng, Y. Chen, W. Xiong, J. Yang, F. Yao, Y. Wu, D. Wang, Y. Hu, and J. Liu. 2016. Assessment of a Flavone-Polysaccharide based prescription for treating duck virus hepatitis. *PLoS One* 11:e146046.
- El-Nekeety, A. A., S. H. Abdel-Azeim, A. M. Hassan, N. S. Hassan, S. E. Aly, and M. A. Abdel-Wahhab. 2014. Quercetin inhibits the cytotoxicity and oxidative stress in liver of rats fed aflatoxin-contaminated diet. *Toxicol. Rep.* 1:319–329.
- Grattagliano, I., L. P. Montezinho, P. J. Oliveira, G. Fruhbeck, J. Gomez-Ambrosi, F. Montecucco, F. Carbone, M. R. Wieckowski, D. Q. Wang, and P. Portincasa. 2019. Targeting mitochondria to oppose the progression of nonalcoholic fatty liver disease. *Biochem. Pharmacol.* 160:34–45.
- Guo Yupu, P. W. 1984. Preliminary identifications of the duck hepatitis virus serotypes isolated in Beijing, China. *Chin. J. Vet. Med. (Zhongguo Shouyi Zazhi)* 11:2–3.
- Holmstrom, K. M., L. Baird, Y. Zhang, I. Hargreaves, A. Chalasani, J. M. Land, L. Stanyer, M. Yamamoto, A. T. Dinkova-Kostova, and A. Y. Abramov. 2013. Nrf2 impacts cellular bioenergetics by controlling substrate availability for mitochondrial respiration. *Biol. Open* 2:761–770.
- Huang, T., Y. Liu, and C. Zhang. 2019. Pharmacokinetics and bioavailability Enhancement of baicalin: a review. *Eur. J. Drug Metab. Pharmacokinet.* 44:159–168.
- Ishfaq, M., C. Chen, J. Bao, W. Zhang, Z. Wu, J. Wang, Y. Liu, E. Tian, S. Hamid, R. Li, L. Ding, and J. Li. 2019. Baicalin ameliorates oxidative stress and apoptosis by restoring mitochondrial dynamics in the spleen of chickens via the opposite modulation of NF-kappaB and Nrf2/HO-1 signaling pathway during *Mycoplasma gallisepticum* infection. *Poult. Sci.* 98:6296–6310.
- Jin, X., Z. Xu, X. Zhao, M. Chen, and S. Xu. 2017. The antagonistic effect of selenium on lead-induced apoptosis via mitochondrial dynamics pathway in the chicken kidney. *Chemosphere* 180:259–266.
- Kamomae, M., M. Kameyama, J. Ishii, M. Nabe, Y. Ogura, H. Iseki, Y. Yamamoto, and M. Mase. 2017. An outbreak of duck hepatitis A virus type 1 infection in Japan. *J. Vet. Med. Sci.* 79:917–920.
- Kang, M., J. H. Roh, and H. K. Jang. 2018. Protective efficacy of a bivalent live attenuated vaccine against duck hepatitis A virus types 1 and 3 in ducklings. *Vet. Microbiol.* 214:108–112.
- Lai, Y., N. Zeng, M. Wang, A. Cheng, Q. Yang, Y. Wu, R. Jia, D. Zhu, X. Zhao, S. Chen, M. Liu, S. Zhang, Y. Wang, Z. Xu, Z. Chen, L. Zhu, Q. Luo, Y. Liu, Y. Yu, L. Zhang, J. Huang, B. Tian, L. Pan, R. M. Ur, and X. Chen. 2019. The VP3 protein of duck hepatitis A virus mediates host cell adsorption and apoptosis. *Sci. Rep.* 9:16783.
- Liu, R., S. Shi, Y. Huang, Z. Chen, C. Chen, L. Cheng, G. Fu, H. Chen, C. Wan, and Q. Fu. 2019. Comparative pathogenicity of different

- subtypes of duck hepatitis A virus in Pekin ducklings. *Vet. Microbiol.* 228:181–187.
- Ludtmann, M. H., P. R. Angelova, Y. Zhang, A. Y. Abramov, and A. T. Dinkova-Kostova. 2014. Nrf2 affects the efficiency of mitochondrial fatty acid oxidation. *Biochem. J.* 457:415–424.
- Moncada, S., and J. P. Bolanos. 2006. Nitric oxide, cell bioenergetics and neurodegeneration. *J. Neurochem.* 97:1676–1689.
- Oo, A., K. Rausalu, A. Merits, S. Higgs, D. Vanlandingham, S. A. Bakar, and K. Zandi. 2018. Deciphering the potential of baicalin as an antiviral agent for Chikungunya virus infection. *Antiviral. Res.* 150:101–111.
- Petrosillo, G., P. Portincasa, I. Grattagliano, G. Casanova, M. Matera, F. M. Ruggiero, D. Ferri, and G. Paradies. 2007. Mitochondrial dysfunction in rat with nonalcoholic fatty liver Involvement of complex I, reactive oxygen species and cardiolipin. *Biochim. Biophys. Acta* 1767:1260–1267.
- Pisoschi, A. M., and A. Pop. 2015. The role of antioxidants in the chemistry of oxidative stress: a review. *Eur. J. Med. Chem.* 97:55–74.
- Shaw, P., and A. Chattopadhyay. 2020. Nrf2-ARE signaling in cellular protection: Mechanism of action and the regulatory mechanisms. *J. Cell Physiol* 235:3119–3130.
- Strom, J., B. Xu, X. Tian, and Q. M. Chen. 2016. Nrf2 protects mitochondrial decay by oxidative stress. *Faseb J.* 30:66–80.
- Surai, P. F., and I. I. Kochish. 2019. Nutritional modulation of the antioxidant capacities in poultry: the case of selenium. *Poult. Sci.* 98:4231–4239.
- Wang, L., M. Pan, Y. Fu, and D. Zhang. 2008. Classification of duck hepatitis virus into three genotypes based on molecular evolutionary analysis. *Virus Genes* 37:52–59.
- Wen, X., D. Zhu, A. Cheng, M. Wang, S. Chen, R. Jia, M. Liu, K. Sun, X. Zhao, Q. Yang, Y. Wu, and X. Chen. 2018. Molecular epidemiology of duck hepatitis a virus types 1 and 3 in China, 2010–2015. *Transbound. Emerg. Dis.* 65:10–15.
- Xiong, W., Y. Chen, Y. Wang, and J. Liu. 2014. Roles of the antioxidant properties of icariin and its phosphorylated derivative in the protection against duck virus hepatitis. *BMC Vet. Res.* 10:226.
- Yugo, D. M., R. Hauck, H. L. Shivaprasad, and X. J. Meng. 2016. Hepatitis virus infections in poultry. *Avian Dis.* 60:576–588.
- Zhang, X., X. Wu, Q. Hu, J. Wu, G. Wang, Z. Hong, and J. Ren. 2019. Mitochondrial DN in liver inflammation and oxidative stress. *Life Sci.* 236:116464.